Tunnelling Corrections in Hydrogen Abstractions by Excited-State Ketones

Monica Barroso, Luis G Arnaut, Sebastiao J Formosinho

Journal of Physical Organic Chemistry

Tunnelling Corrections in Hydrogen Abstractions by Excited-State Ketones

Journal:	*Journal of Physical Organic Chemistry*
Manuscript ID:	POC-09-0282.R1
Wiley - Manuscript type:	Research Article
Date Submitted by the Author:	15-Feb-2010
Complete List of Authors:	Barroso, Monica; Imperial College London, Department of Chemistry; University of Coimbra, Chemistry Department Arnaut, Luis; University of Coimbra, Chemistry Department Formosinho, Sebastiao; University of Coimbra, Chemistry Department
Keywords:	tunnelling, ISM, ketone photochemistry, hydrogen abstraction

Tunnelling Corrections in Hydrogen Abstractions by Excited-State Ketones

Monica Barroso, Luis G. Arnaut, Sebastião J. Formosinho[*]

Department of Chemistry, University of Coimbra, 3004-535 Coimbra, Portugal

E-mail: sformosinho@qui.uc.pt

Abstract: Hydrogen abstraction from 1-phenylethanol by triplet acetophenone occurs from both C-H and O-H bonds. The reaction path of the Interacting-State Model (ISM) is used with the Transition-State Theory (TST) and the semiclassical correction for tunnelling (ISM/scTST) to help rationalizing the experimental kinetic results and elucidate the mechanisms of these reactions. The weak exothermicity of the abstraction from the strong O-H bond is compensated by electronic effects, hydrogen bonding and tunnelling, and is competitive with the more exothermic abstraction from the α-C-H bond of 1-phenylethanol. The alkoxy radical formed upon abstraction from O-H reacts within the solvent cage and the primary product of this reaction is 1-phenylethenol. The corresponding kinetic isotope effect is ca. 3 and is entirely consistent with a tunnelling correction ca. 9 for H abstraction. We therefore demonstrate that the tunnelling correction is the major contributor to the kinetic isotope effect.

Keywords: tunnelling, intersecting-state model; ketone photochemistry; hydrogen abstraction

Introduction

The photochemistry of ketones is particularly well known [1] and is often used in textbook examples of photochemical reactions [2]. Aromatic ketones have been of interest to photochemists because they usually form triplet states in less than 1 ns with nearly unity quantum yields, and such triplet states are sufficiently long-lived to have a rich reactivity. A very common reaction of excited ketones in the presence of substrates with activated CH bonds, such as alcohols, is the hydrogen-atom abstraction from the $^3(n,\pi^*)$ state of the ketone. Over 30 years ago one of us proposed that tunnelling should play a major role in the mechanism of photochemical H-abstractions [3, 4]. Here we present new data on such reactions and include them in the general approach recently developed for the calculation of H-transfer rates in a very wide variety of systems, from gas phase to solution and to enzymes [5-9]. Thus, it is not our intention to review the controversies in the literature on the adequacy of thermal activation versus nuclear tunnelling models in the description of photochemical H-abstractions. We note, however, that the criticism of nuclear tunnelling is often based on the observation of temperature dependences following linear Eyring [10] or Arrhenius plots [11], although vibrationally-assisted tunnelling also yields such linear plots above 200 K [12].

We made a detailed investigation of the H-atom abstraction reaction from 1-phenylethanol (PE) by acetophenone (AP) because it presents a mechanistic challenge that can only be solved with a sound knowledge of the kinetics and thermodynamics of H-atom transfers. The mechanistic challenge is the unexpected inefficient of this H-abstraction: the quantum yields for pinacol formation in this system do not exceed 50% in benzene, contrary to analogous H-abstractions by benzophenone [13]. Competitive H-abstraction from the OH group was invoked to explain this observation [14, 15]. In Scheme 1 it is assumed that the in-cage disproportionation of the triplet α-hydroxy–alkoxy radical pair leads to the triplet acetophenone enol [16]. The escape of the alkoxy radical from the solvent cage can be excluded because it would rapidly react with more

PE, generate another hemipinacol radical and eventually contribute to increase the product quantum yield.

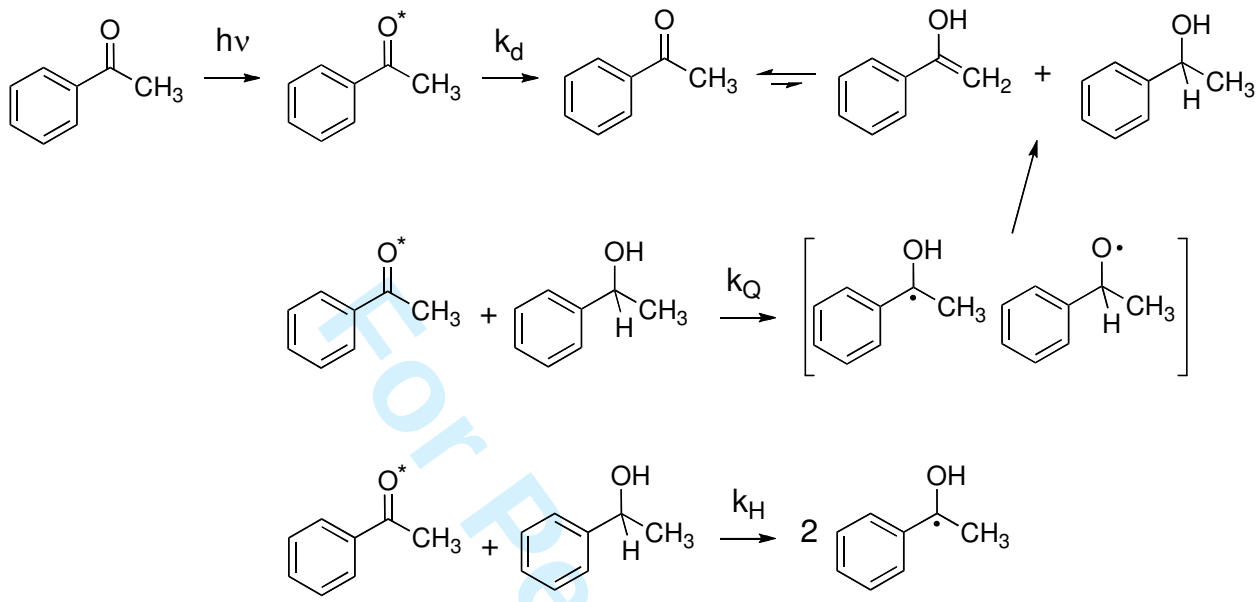

Scheme 1. Mechanism of competitive H-abstraction from CH or OH bonds of 1-phenylethanol by acetophenone.

To explore this mechanism and understand the role of tunnelling on the photoreduction of AP by PE, we have used nanosecond laser flash photolysis to determine the rates of acetophenone triplet deactivation, and photoacoustic calorimetry (PAC) to measure the enthalpies of the H-atom abstraction reactions. The data are interpreted with the Intersecting/Interacting-State Model (ISM) associated with semi-classical TST rate calculations (ISM/scTST) [5, 9, 17, 18]. ISM is a semi-empirical reactivity model that deals in a compact manner with the chemical bonds that are broken and formed in a chemical reaction, characterizing them by their Morse potentials and equilibrium bond-lengths, and associates their interactions along a unidimensional reaction coordinate with the reaction energy and an electronic parameter. ISM uses only a small number of effective parameters, which favours the "human understanding" of reactive processes and

provides valuable insight into the factors that control chemical reactivity, namely nuclear tunnelling.

Experimental

Acetophenone and 1-phenylethanol (Aldrich) were distilled at low pressure. Benzene and acetonitrile were purified by standard procedures. O-deuterated 1-phenylethanol was obtained adding D_2O to previously distilled 1-phenylethanol. The mixture was stirred and, after separation, the aqueous phase was extracted. This procedure was repeated several times and the relative amount of deuterated 1-phenylethanol was monitored by IR spectroscopy. The final mixture, containing 85% of O-deuterated compound was dried and distilled at low pressure before use.

Transient absorption experiments were performed with an Applied Photophysics LK.60 laser flash photolysis spectrometer with a Spectra Physics Quanta-Ray GCR-130 Nd:YAG laser and a Hewlett-Packard Infinium oscilloscope. The excitation wavelength used in this work was 355 nm for all the experiments. Before measurements, the solutions were purged with N_2 for 20 minutes.

Time-resolved PAC measurements were performed in a homemade apparatus following the front-face irradiation design described by Arnaut *et al* [19]. The solutions were pumped through a 0.11 mm thick cell at a 1 ml/min flow with a SSI chromatography pump, and irradiated with an unfocused N_2 laser (337 nm, 1.0 mJ/pulse) working at the frequency of 2.0 Hz. More than 99% of the light impinging on the front face dielectric mirror is reflected back in the solution, thus minimizing the background signal. A small fraction of the laser beam was deflected to a photodiode in order to trigger the digital storage oscilloscope (Tektronix DSA 601,1 Gs/s, two channels). The acoustic waves were detected with a 2.25 MHz Panametrics transducer (model A106S) and pre-amplified with a Panametrics ultrasonic amplifier (model 5676). Sample and reference solutions were matched to better than 1% absorbances at the irradiation wavelength. 2-

Hydroxybenzophenone was used as photoacoustic reference. Samples were deoxygenated by bubbling with a gentle flow of solvent-saturated nitrogen.

ISM/scTST Calculations

The breaking of an A-H bond and the formation, in a synchronous manner, of another bond B-H can be written

$$AH + B \rightarrow BH + A \qquad (I)$$

Along the reaction coordinate there is a rising of the potential energy up to the transition state (TS) followed by a decrease. The reaction energy barrier is controlled by the energy of TS with respect to that of reactants, but in order to properly assess quantum mechanical tunnelling and kinetic isotope effects (KIE) one requires the entire barrier shape. We recently developed a semi-empirical model that gives barrier shapes in very good agreement with those of *ab initio* calculations for small systems, but that can be employed to calculate the barriers of polyatomic systems without added difficulty. This model, named Intersecting/Interacting State Model (ISM), has been described in detail elsewhere [5-9, 17, 18, 20-22]. Here we present only a brief description of ISM with emphasis on the factors that contribute to tunnelling corrections.

ISM is based on three fundamental assumptions. The first one is the concept of bond-order conservation along the reaction coordinate, provided by the BEBO model of Johnston and Parr [23],

$$n = n_{HB} = 1 - n_{HA} \qquad (1)$$

where n_{HB} is the bond order of the new bond formed in the products and n_{HA} is the bond order of the bond that is broken in the reactants. The bond order is used in ISM to make a linear

interpolation between the Morse curves of HA and HB, V_{HA} and V_{HB}, along the reaction coordinate

$$V_{cl}(n) = (1-n)V_{HA} + nV_{HB} + n\Delta V^0 \quad (2)$$

where $V_{cl}(n)$ represents the classical path of the ISM and ΔV^0 is the reaction energy.

The second assumption of ISM is based on the Pauling relation between bond lengths and bond orders [24], generalized to transition states

$$\begin{aligned} l^{\ddagger}_{HA} - l_{HA,eq} &= -a'_{sc}\left(l_{HA,eq} + l_{HB,eq}\right)\ln\left(n^{\ddagger}_{HA}\right) \\ l^{\ddagger}_{HB} - l_{HB,eq} &= -a'_{sc}\left(l_{HA,eq} + l_{HB,eq}\right)\ln\left(n^{\ddagger}_{HB}\right) \end{aligned} \quad (3)$$

where a'_{sc} is a "universal" constant, to relate transition state bond lengths ($l^{\ddagger}$) to the corresponding bond orders ($n^{\ddagger}$) and to the equilibrium bond lengths of reactants and products ($l_{HA,eq}$ and $l_{HB,eq}$). The value of a'_{sc} was obtained from the bond extension from the potential energy surface of $H+H_2$ system [25], a'_{sc}=0.182.

The last assumption concerns the electronic stabilization when A, H, and B interact at the transition state, A···H···B. The electrophilicity index m proposed by Parr [26] represents the saturation point for electron inflow as the ratio between the negative of the electronic chemical potential, μ_{el}, and the chemical hardness, η_{el}, and is a good measure for the extra electronic stabilization of the transition state,

$$m = \frac{-\mu_{el}}{\eta_{el}} = \frac{I_P + E_A}{I_P - E_A} \quad (4)$$

where I_P is the ionization potential and E_A is the electron affinity of A or B. It increases with the propensity of the "ligands" A and B to participate in charge redistribution in the transition state (low I_P and/or high E_A), but otherwise leads to no stabilization (high I_P and/or low E_A). The electronic saturation further stabilizes the transition state and was introduced in the ISM reaction coordinate through a modification of the reactant and product Morse curves

$$V_{\mathrm{HA}} = D_{\mathrm{e,HA}} \left\{1 - \exp\left[\beta_{\mathrm{HA}} \Delta l_{HA} / m\right]\right\}^2$$
$$V_{\mathrm{HB}} = D_{\mathrm{e,HB}} \left\{1 - \exp\left[\beta_{\mathrm{HB}} \Delta l_{HB} / m\right]\right\}^2 \quad (5)$$

where $D_{\mathrm{e,HA}}$ and $D_{\mathrm{e,HB}}$ are the electronic dissociation energies, β_{HA} and β_{HB} the spectroscopic constants of the bonds HA and HB.

The assumptions discussed above suffice to determine the classical reaction path of ISM. However, zero-point energies (ZPE) and tunnelling may substantially influence the rates of H-atom transfers even at room temperature. We obtain the vibrationally-adiabatic reaction path adding ZPE to the classical reaction path,

$$V_{ad}(n) = V_{cl}(n) + \sum_i \left(\frac{1}{2} hc\bar{\nu}_i\right) \quad (6)$$

where $\bar{\nu}_i$ are the vibration frequencies of the normal modes orthogonal to the reaction coordinate. The ZPE of the reactants in given by the vibrational frequency of the AH bond, and that of the products is the vibrational frequency of the BH bond. The frequencies of the linear triatomic transition state $\{A\cdots H\cdots B\}^{\ddagger}$ were estimated from Wilson's equation with the neglect of the interaction between bending and stretching [27], and using the fractional bonds $\{A\cdots H\}^{\ddagger}$ and $\{H\cdots B\}^{\ddagger}$. The linear relation between symmetric stretching and bending frequencies in triatomic systems is employed to estimate the bending frequency from the symmetric stretching frequency [5]. The vibrations of the AH and BH bonds in the reactants and products become the asymmetric stretching of the transition state, which has an imaginary frequency and, for symmetric systems (A=B), corresponds to the curvature of the reaction path at the transition state. Thus, in these conditions, the ZPE contribution of the AH and BH bonds is lost at the transition state. On the other hand, the symmetric stretching of $\{A\cdots H\cdots B\}^{\ddagger}$, and the bending scaled to this stretching, is lost in the reactants and products. A switching function was introduced to provide the correct asymptotic limits of these contributions to the ZPE [5].

The reduced mass of the asymmetric stretch at the transition state is also the mass required

for the tunnelling correction. When the force constants of the AH and BH are identical, this reduced mass can be written

$$\mu = \frac{2}{\mu_A + 2\mu_H + \mu_B + \sqrt{\left(\mu_A - \mu_B\right)^2 + 4\mu_H^2}} \tag{7}$$

where $\mu_i = m_i^{-1}$. When the masses of A and B are much larger than that of H, which is approximately the case of the systems discussed in this work, the equation above reduces to $\mu = (2/m_H)^{-1}$. With such low reduced masses, we can expect the prevalence of tunnelling in H-atom transfers.

ISM/scTST calculations employ the semiclassical approximation to calculate tunnelling corrections along the vibrationally-adiabatic path. Following this approximation, the transmission coefficient and transmission probabilities are [28],

$$\kappa(T) = 1 + \frac{2}{k_B T}\int_{\varepsilon_0}^{\Delta V_a^{\ddagger}} \sinh\left(-\frac{\Delta V_a^{\ddagger} - \varepsilon}{k_B T}\right) G(\varepsilon)\,\mathrm{d}\varepsilon \tag{8}$$

$$\begin{aligned} G(\varepsilon) &= \left\{1 + \exp\left[2\gamma(\varepsilon)\right]\right\}^{-1} && \varepsilon_0 \le \varepsilon \le \Delta V_a^{\ddagger} \\ &= 1 - G\left(2\Delta V_a^{\ddagger} - \varepsilon\right) && \Delta V_a^{\ddagger} \le \varepsilon \le \left(2\Delta V_a^{\ddagger} - \varepsilon_0\right) \\ &= 0 && \left(2\Delta V_a^{\ddagger} - \varepsilon_0\right) < \varepsilon \end{aligned} \tag{9}$$

respectively, where the barrier penetration integral is given by

$$\gamma(\varepsilon) = \frac{2\pi}{h}\int_{s_<}^{s} \sqrt{2\mu\left[V_a(s) - \varepsilon\right]}\,\mathrm{d}s \qquad \varepsilon < \Delta V_a^{\ddagger} \tag{10}$$

The threshold energy is the limiting value of the vibrationally-adiabatic potential energy for exothermic or endothermic reactions

$$\varepsilon_0 = \max\left[V_a(s = -\infty), V_a(s = +\infty)\right] \tag{11}$$

The reduced mass is given by Eq. (7), the reaction coordinate s is defined in terms of bond extensions as

$$s = -\sqrt{\left(l_{BC} - l_{BC}^{\ddagger}\right)^2 + \left(l_{AB} - l_{AB}^{\ddagger}\right)^2} \qquad l_{BC} \le l_{BC}^{\ddagger}$$
$$s = +\sqrt{\left(l_{BC} - l_{BC}^{\ddagger}\right)^2 + \left(l_{AB} - l_{AB}^{\ddagger}\right)^2} \qquad l_{BC} > l_{BC}^{\ddagger} \tag{12}$$

and is related to the reaction coordinate expressed in terms of bond order by Eq. (3). Finally, $s_>$ and $s_<$ are the classical turning points, i.e., the locations at which $V_a(s)=\varepsilon$.

The semiclassical TST formulation for a bimolecular rate constant in the gas phase is [29]

$$k = \kappa(T)\frac{k_B T}{h}\frac{Q_{\ddagger}}{Q_{AH}Q_B}\exp\left(-\frac{\Delta V_{ad}^{\ddagger}}{RT}\right) \tag{13}$$

where $\Delta V_{ad}^{\ddagger}$ is the maximum along the vibrationally-adiabatic path with respect to the reactants, $\kappa(T)$ is the tunnelling correction, and $Q_{\ddagger}$, Q_{AH} and Q_B are the partition functions of the transition state and reactants, respectively. The simplification achieved by ISM/scTST calculations of polyatomic systems is based on the conservation of ZPE of spectator modes along the reaction coordinate, which also implies the cancellation of factors in the ratio of partition functions. When the typical ratio of vibrational to rotational partition functions is included in the pre-exponential factor, we obtain a simplified expression valid for bimolecular reactions between polyatomic reactants in solution [17], per equivalent H-atom,

$$k = \kappa(T)\frac{k_B T}{h}\left(\frac{1}{3}\right)^3\frac{Q_{AHB^{\ddagger}}}{Q_B Q_{HA}}\exp\left(-\frac{\Delta V_{ad}^{\ddagger}}{RT}\right) \tag{14}$$

The expression above needs to be modified when H-bonded complexes are present along the reaction coordinate. In such cases, the H-atom transfer occurs along the H-bond and the frequency of reaction is that of the H-bond. The energy, frequency ($\omega_{e(AB)}$) and bond lengths of the H-bonded complex are described by the Lippincott-Schroeder potential [30], that needs only one of these parameters to calculate the others. The expression for the rate constant in H-bonded system is [17]

$$k = \kappa(T) c\,\omega_{e(AB)} K_c \exp\left(-\frac{\Delta V_{ad}^{\ddagger}}{RT}\right) \tag{15}$$

where K_c is the fraction of H-bonded systems.

ISM/scTST rate calculations only require the reactions energy, the Morse potentials and bond lengths of the reactive bonds and the electronic parameters (ionization potential and electron affinity) of the radicals formed. In H-bonded systems, the energies of the H-bonded complexes must also be included in the reaction coordinate. With these data, the calculations take less than a second per temperature. An Internet free-access site developed for ISM/scTST calculations [31] was used for all the rate calculations presented here.

Results and Discussion

Kinetics

Figure 1 shows the triplet-triplet absorption spectra of acetophenone (AP) in acetonitrile and benzene upon laser excitation with the second harmonic of a Nd:YAG laser. The spectra are characterized by strong absorption bands in the UV, with maxima around 310 nm and 320 nm, in benzene and acetonitrile, respectively. Additionally, a weaker absorption band is observed with maxima at 400-420 nm in benzene. The latter feature is consistent with a (n,π*) lowest triplet state, usually observed in non-polar solvents [32]. Due to the proximity between (n,π*) and (π,π*) lowest triplets in acetophenone, a change in the polarity of the solvent may invert the order of these states and hence affect the reactivity of acetophenone.

The triplet lifetimes obtained from the decays of triplet absorption were 1.8 μs in benzene and 1.3 μs in acetonitrile. Although slightly lower than the values reported in literature,[33, 34] possibly due to quenching by residual oxygen present in the solutions, these values confirm a long triplet lifetime in non-polar and un-reactive solvents.

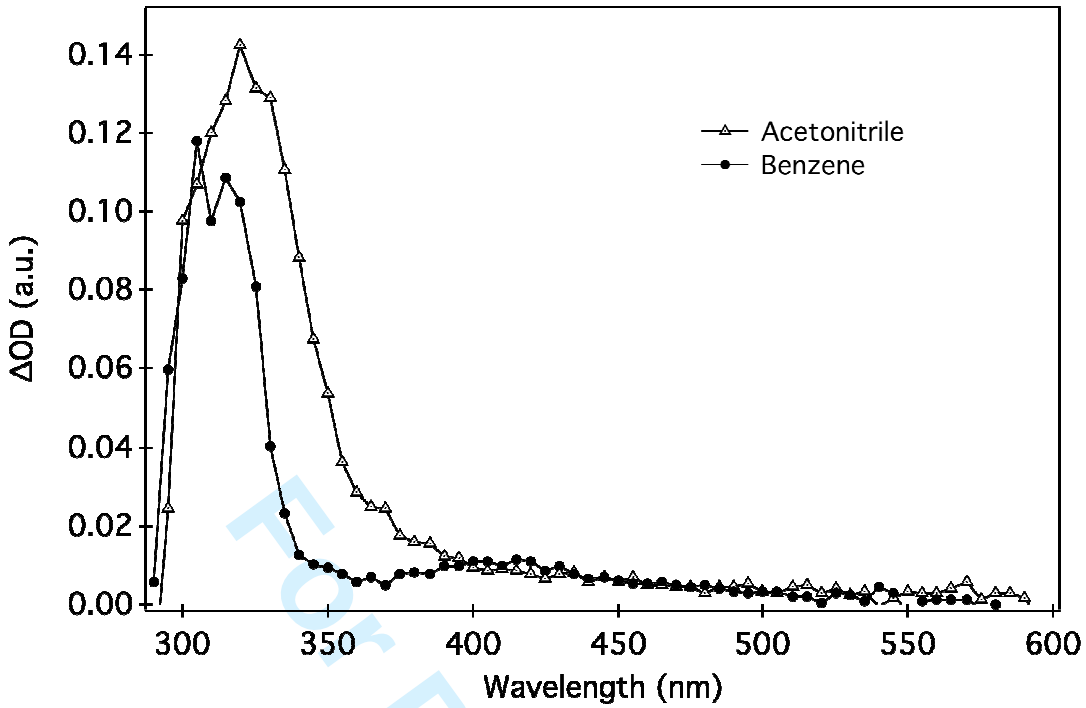

Figure 1. Transient absorption spectra of acetophenone (17 mM) degassed solution of benzene (—) and acetonitrile (····) 100 ns after laser excitation at 355 nm.

In the presence of excess 1-phenylethanol the transient absorption bands corresponding to the α-phenylmethyl radical are observed (Figure 2). The interpretation of these results is complicated by the overlap of the absorptions of triplet acetophenone and the radical [32]. To minimize this problem, the kinetic analysis was based on decays probed at 330 nm and 340 nm, for benzene and acetonitrile solutions respectively.

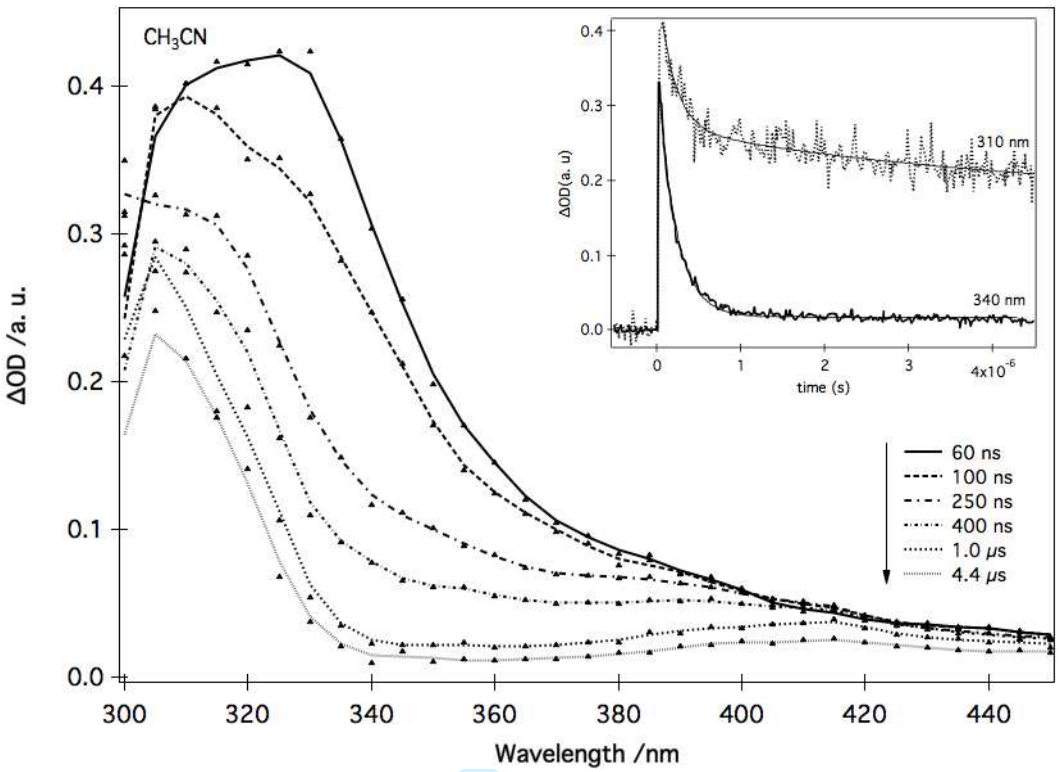

Figure 2. Transient absorption spectra of acetophenone (19.7 mM) in the presence of 1-phenylethanol (0.095M), in acetonitrile. The inset compares the decays probed at 310 nm, where triplet acetophenone and radical bands overlap, and 340 nm, where the triplet is the predominant transient species. Laser excitation at 355 nm.

According to Scheme 1, the rate of decay of ^{3}AP can be described by

$$k_{obs} = k_d + k_r[PE] \qquad (8)$$

where $1/k_d$ represents the natural triplet lifetime and k_r is the overall rate of hydrogen atom abstraction, which can be further decomposed into k_H+k_Q, the rates of H-atom abstraction from the CH and OH bonds in 1-phenylethanol, respectively. The values of k_d and k_r can be obtained from the intercept and slope of the plot of k_{obs} against the concentration of 1-phenylethanol (Figure 3a). To further understand the role of the OH bond in this mechanism, we have studied the reaction of AP with O-deuterated 1-phenylethanol (PE-OD), as shown in Figure 3b. The rates of H-atom abstraction from the deuterated compound are slower in both solvents, resulting in an

overall kinetic isotope effect of 1.5 and 1.4 for benzene and acetonitrile, respectively. Table 1 summarizes the flash photolysis data.

Table 1. Summary of flash photolysis results for the photoreduction of acetophenone by 1-phenylethanol and O-deuterated 1-phenylethanol, in benzene and acetonitrile.[a]

	C_6H_6	CH_3CN
τ_T / μs	1.8	1.3
k_r /10^6 $M^{-1}s^{-1}$	6.0	5.2
k_H /10^6 $M^{-1}s^{-1}$	3.5 [b]	2.6 [b]
k_Q /10^6 $M^{-1}s^{-1}$	2.5 [b]	2.6 [b]
k_r (D) /10^6 $M^{-1}s^{-1}$	4.1 [c]	3.8 [c]
k_H (D) /10^6 $M^{-1}s^{-1}$	-	2.7
k_Q (D) /10^6 $M^{-1}s^{-1}$	-	1.1
KIE	1.5	1.4

[a] [AP] = 20 mM; [PE] and [PE-OD] varied from 0 to 1.5 M; [b] Calculated with the literature quantum yields of the H-atom abstractions [14, 15]; [c] Rate values corrected for 100% deuteration of PE.

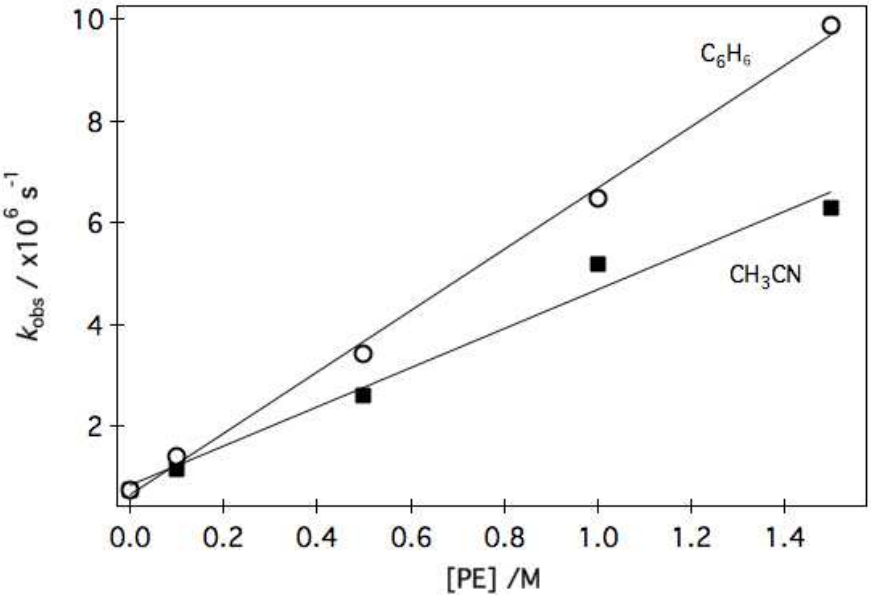

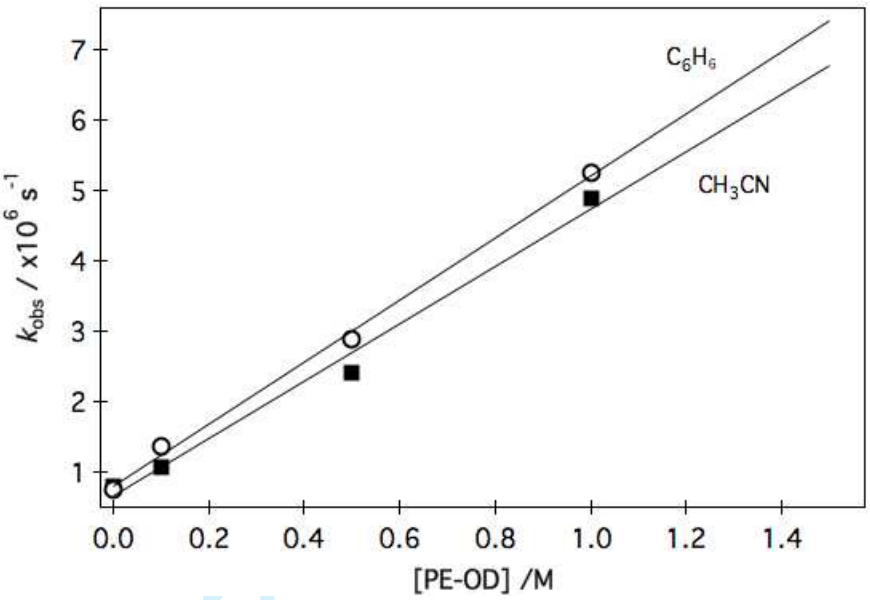

Figure 3. Dependence of the observed rate constants for acetophenone triplet absorption decay on the concentration of 1-phenylethanol (upper plot) and O-deuterated 1-phenylethanol (lower plot).

Wagner and co-workers have shown that the maximum quantum yield for acetophenone photoreduction by 1-phenylethanol is 0.59 in benzene and 0.50 in acetonitrile [14, 15]. Based on this information we calculated the values of k_H and k_Q presented in Table 1. These authors further showed that the photoreduction quantum yield increases to 0.70, in acetonitrile, upon O-deuteration of 1-phenylethanol. Taking this information we estimate the rate of H-abstraction from CH, $k_H(D) = 2.7x10^6$ $M^{-1}s^{-1}$. When comparing this value with the rate of H-atom abstraction from CH in AP/PE system, $k_H(H) = 2.6x10^6$ $M^{-1}s^{-1}$, we obtain KIE(H)=0.96, which shows that O-deuteration only affects the rate of H-atom abstraction from the OH bond. The actual KIE for the quenching by the OH/OD bond is KIE(Q)=2.4.

Quenching by the OH bond exhibits a KIE that is consistent with that of a H-abstraction reaction, but does not lead to isolated products. The primary product resulting from H-abstraction from the OH group is a triplet α-hydroxy–alkoxy radical pair, Scheme 1. The absence of products originating from these radicals implies their involvement in a very fast reaction, competitive with

the escape from the solvent cage. Scheme 2 gives a detail of the overall mechanism, where the alkoxy radical abstracts an H-atom from the α-hydroxy radical. The subsequent decay of the 1,2-biradical is expected to be fast because the triplet acetophenone enol can also be regarded as a 1,2-biradical and its lifetime is expected to be less than 10 ns [35]. Thus, the triplet α-hydroxy–alkoxy radical pair leads quantitatively to 1-phenylethenol that slowly isomerizes to acetophenone [36]. This isomerisation is favoured by an enthalpy change of –10 kcal/mol [37].

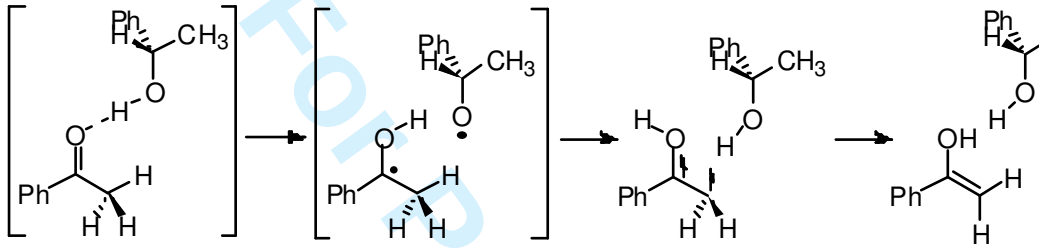

Scheme 2. Detail of the quenching mechanism via H-abstraction from the OH bond.

Thermochemistry

The H-abstraction from the OH bond leads to PE and 1-phenylethenol, which is concomitant with the formation of a pair of identical 1-phenyl-1-hydroxyethyl radicals via H-abstraction from the CH bond. As illustrated in Scheme 3, heat released in this process is given by

$$E_{h\nu}\phi_2 = \Phi_H\left(-\Delta H_H\right) + \Phi_Q\left(-\Delta H_Q\right) + (1 - \Phi_H - \Phi_Q)E_T \qquad (9)$$

where ΔH_{H} is the enthalpy of the abstraction from the CH bond, ΔH_{Q} is the enthalpy of the transformation of triplet acetophenone in 1-phenylethenol, and the last term accounts for the decay of triplet states that did not react with PE. This transient heat release, and the precedent heat released in the formation of the triplet state of acetophenone, is conveniently measured by photoacoustic calorimetry (PAC).

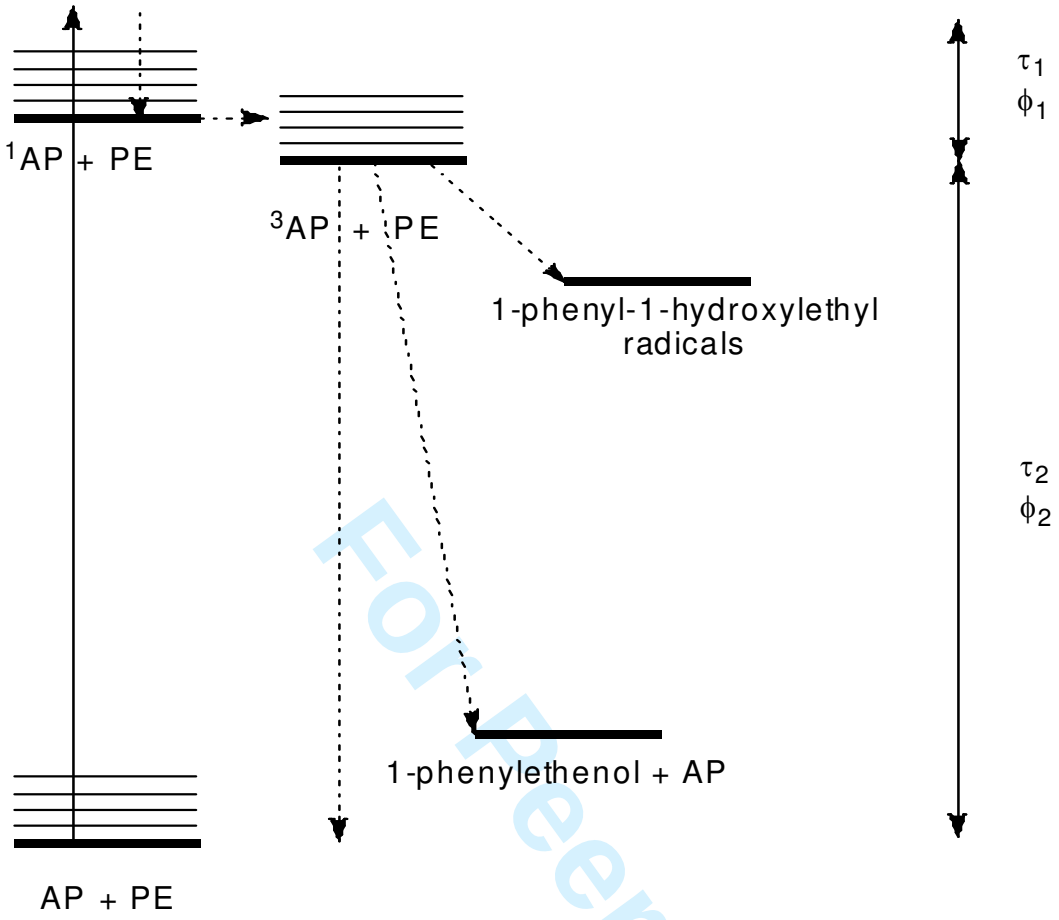

Scheme 3. Energy relations in photoacoustic calorimetry.

Time-resolved photoacoustic calorimetry distinguishes the prompt heat released in the formation of a triplet state of an aromatic ketone from the subsequent heat released in the reactions of that triplet state [38]. Table 2 shows the results of the analysis of the PAC waves obtained for the AP/PE system in benzene after laser excitation at 337 nm. The experimental data were analyzed using a biexponential decay fixing τ_1=1 ns and fitting simultaneously ϕ_1, τ_2 and ϕ_2 with an analytical deconvolution method [16]. The presence of biphotonic absorption required additional experiments in the same conditions but different laser intensities, and extrapolation of ϕ_1, τ_2 and ϕ_2 to zero laser intensity. The biexponential analysis of experimental PAC waves, setting τ_1=1 ns, gives ϕ_1 = 0.147 in the absence of PE after extrapolation to zero laser intensity. From the extrapolated value of ϕ_1, the triplet quantum yield of unity for acetophenone, and the

excitation laser energy for 337 nm, E_{hv}=84.8 kcal/mol, the triplet state energy can be calculated as $E_T = E_{hv}(1-\phi_1)$=73.2 kcal/mol, in good agreement with the 74 kcal/mol reported in the literature for non-polar solvents [34]. Typically the uncertainty in the fractions of energy release (ϕ_1 and ϕ_2) is less than ±0.03, which correspond to less than ±2.5 kcal/mol uncertainty.

Table 2. Parameters obtained in the analytical deconvolution of the PAC waves generated in the decay of acetophenone in the presence of 1-phenylethanol, in benzene.

[PE] (M)	C_6H_6		
	ϕ_1	τ_2 (ns)	ϕ_2
0	0.147	–	–
0.08	0.113	*1855*	*2.12*
0.10	0.102	*1161*	*1.62*
0.20	0.131	845	1.28
0.50	0.154	411	0.91
1.0	0.136	462	0.50
2.0	0.174	253	0.47

The enthalpy of the overall reaction of AP with PE reaction can also be derived from PAC experiments, by extrapolating ϕ_2 to infinite quencher concentration, in which case we have $\Delta H_r = -\phi_2^{\infty} \cdot E_{hv}$, $\Delta H_r = \Phi_H \Delta H_H + \Phi_Q \Delta H_Q$ and $\Phi_H + \Phi_Q = 1$. As shown in Figure 4, the extrapolation to [PE]=∞ gives ϕ_2^{∞}= 0.50, and we calculate ΔH_r=–42.4 kcal/mol. The consistency between this value and the estimate of ΔH_r expected from the concomitant generation of 1-phenyl-1-hydroxyethyl radicals and 1-phenylethenol requires information on the quantum yields Φ_H and Φ_Q and heats of reaction ΔH_H and ΔH_Q. The heats of formation of PE and of the 1-phenyl-1-hydroxyethyl radical are not known but the reaction enthalpy of the H-abstraction in the AP/PE system can be obtained from the thermochemical cycle shown in Figure 5.

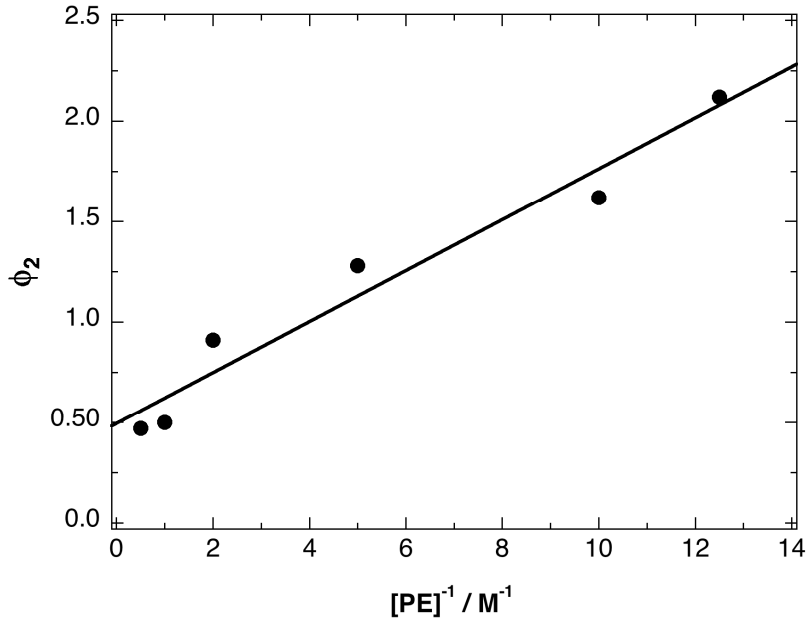

Figure 4. Dependence of the heat released in the interaction between ^{3}AP and PE in benzene on the reciprocal of the concentration of PE.

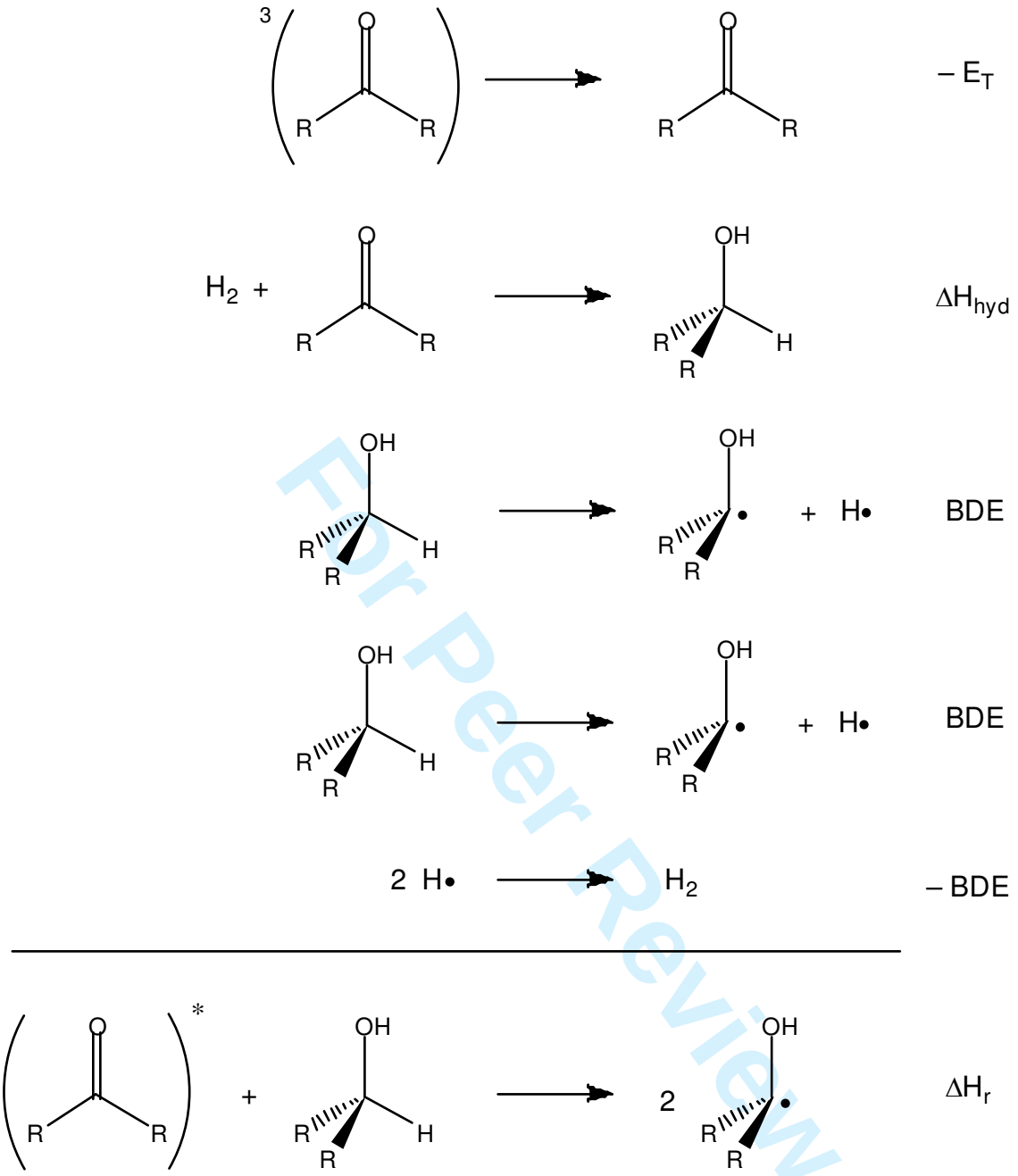

Figure 5. Thermochemical cycle employed to calculate the heats of H-abstraction reactions from CH bonds.

The $R_2C{=}O$ hydrogenation enthalpy is given by the difference in enthalpies of formation of $R_2C{=}O$ and R_2CHOH. Table 3 presents the literature data on the enthalpies of formation of benzophenone and benzhydrol in benzene, and of acetone and 2-propanol in the gas phase. In both cases the heats of hydrogenation are ΔH_{hyd}=–13±1 kcal/mol, and this value can also be taken for the hydrogenation of the C=O bond of AP. The CH bond dissociation energy of PE can be

estimated from that of 2-phenylpropane knowing the energetic stabilization induced by OH with respect to the CH_3. As shown in Table 3, the OH energetic stabilization is the same within experimental error in 2-methylpropane/2-propanol and in 1,1-diphenylethane/benzhydrol. With the data in that table, we estimate that the BDE of PE is 78.9 kcal/mol. With E_T=73.2 kcal/mol, ΔH_{hyd}=–13 kcal/mol and BDE(PE)= 78.9 kcal/mol, we calculate ΔH_H=–32.6 kcal/mol for the triplet state H-atom abstraction of PE by AP. On the other hand, the value of ΔH_Q is simply given by the triplet energy of AP and the isomerisation energy of 1-phenylethenol to acetophenone [36], ΔH_Q=–63.2 kcal/mol. Given the values of Φ_H and Φ_Q reported by Wagner and co-workers in benzene, we estimate ΔH_r=–45 kcal/mol, in good agreement with the experimental value of –42.4 kcal/mol measured in this work. This strongly supports the proposed mechanism and provides thermodynamic data for the calculation of rate constants with ISM.

Table 3. Thermochemical data employed to estimate the BDE of PE and the hydrogenation energy of the C=O in ketones.

	Bond dissociation energies (kcal mol^{-1})		ΔBDE (kcal mol^{-1})
	R=CH_3	R=OH	
$(CH_3)_2CHR$	96.6 [a]	91.1 [a]	5.6
$(Ph)(CH_3)CHR$	84.4 [a]		
$(Ph)_2CHR$	81.0 [a]	75.4 [b]	5.5
	ΔH_f(ketone)	ΔH_f(alcohol)	ΔH_{hyd}
$(CH_3)_2C{=}O \rightarrow (CH_3)_2CHOH$	–52.2 [c]	–65.2 [c]	–13.0
$(Ph)_2C{=}O \rightarrow (Ph)_2CHOH$	–5.2 [b]	–18.0 [b]	–12.8

[a] Ref. [39]. [b] In benzene, ref. [38]. [c] Ref. [40].

Tunnelling

ISM calculations of H-abstraction reactions require the knowledge of the reaction energy, of the parameters describing the Morse potentials of the reactive bonds and the ionization potentials and electronic affinities of the radicals formed [5, 9, 18]. The parameters of the CH bond in PE are taken from the CH in acetaldehyde and those of the OH in the 1-phenyl-1-hydroxyethyl radical are taken from methanol, Table 4. The products are carbon-centred radicals, thus only the electronic parameters of CH_3**C**•O are relevant: such parameters lead to m=1.129. Using the Internet free-access site developed for ISM/scTST calculations [31], we calculate k_{CH} = 9.5x10^5 M^{-1} s^{-1} with ΔH_H=–32.6 kcal/mol, in good agreement with the experimental value of k_H = 3.5x10^6 M^{-1} s^{-1} in benzene. These calculations include a tunnelling correction of 3.1.

Table 4. Bond lengths, bond dissociation energies, vibrational frequencies of the molecules, and ionization potentials and electron affinities of the radicals employed in the calculation of the energy barriers.[a]

	l_{eq} (Å)	D^0_{298} (kcal mol^{-1})	ω_e (cm^{-1})	I_P (eV)	E_A (eV)
CH_3**C**HO	1.128	89.3	2822	7.00	0.423
CH_3**O**H	0.9451	104.2	3681	10.72	1.57

[a] Boldface letters indicate where the radical is centred after the bond to the hydrogen atom is broken; data from ref. [9].

An estimate of the reaction enthalpy for the H-abstraction from the OH bond, can be obtained replacing one BDE(CH) in Figure 5, by the BDE of the OH bond of methanol in Table 4, which leads to ΔH_O=–7.3 kcal/mol. In this case, both carbon- and oxygen-centred radicals are formed and the electronic parameters of both CH_3**C**•O and CH_3**O**• must be included in the

calculation; this increases the electrophilicity index to m=1.578. Additionally, it is known that the transfer of an H-atom between oxygen atoms of neutral species takes place along an H-bond of ca. 2 kcal/mol [6, 17]. With this reaction energy, electrophilicity index, H-bond energies and the Morse parameters of the OH bond in methanol, we still need K_c to calculate k_{OH}. The fraction of H-bonded PE-AP dimers is certainly much smaller than unity, but difficult to estimate. In order to reproduce the experimental rate k_Q = 2.6x10^6 M^{-1} s^{-1} in acetonitrile, we have to set K_c=10^{-3} M^{-1}, which is not an unreasonable estimate and brings the pre-exponential factor for CH and OH abstractions to comparable values. The loss of exothermicity with respect to the H-abstraction from the CH bond is compensated by the increase of the electrophilicity index, that substantially stabilises the transition state. The presence of the H-bond also contributes to reduce the barrier for H-atom abstraction between O-atoms.

The calculation of the KIE for the OH/D abstraction requires the frequency of the OD bond in methanol, which is reported as ω_e=2718 cm^{-1}[41]. On the other hand, it is reasonable to assume that OH and OD abstractions have similar pre-exponential factors and the KIE can be calculated from the ration of ISM/scTST rates for these two systems. With ω_e=2718 cm^{-1} and the other parameters of methanol in Table 4, we calculate a KIE of 3.3, in good agreement with the experimental value of KIE(Q)=2.4. Remarkable, the tunnelling correction is reduced from 8.6 for OH to 3.2 for OD abstraction and is the major contributor to the observed KIE. Deuteration also changes ZPE corrections, that are reduced from $\Delta V_{cl}^{\ddagger}$–$\Delta V_{ad}^{\ddagger}$=1.4 kcal/mol for OH abstraction to 1.0 kcal/mol for OD abstraction. The loss of ZPE is only an important contributor to KIE in symmetrical systems.

Figure 6 presents the reaction paths for the H-abstractions from OH and CH bonds. The reaction barriers are $\Delta V_{ad}^{\ddagger}$=4.9 and 5.8 kcal/mol for the abstractions from the CH and OH bonds respectively. The much higher tunnelling correction calculated for the abstraction from the OH

bond can be ascribed to the much thinner barrier that results from the presence of H-bonded complexes along the reaction coordinate.

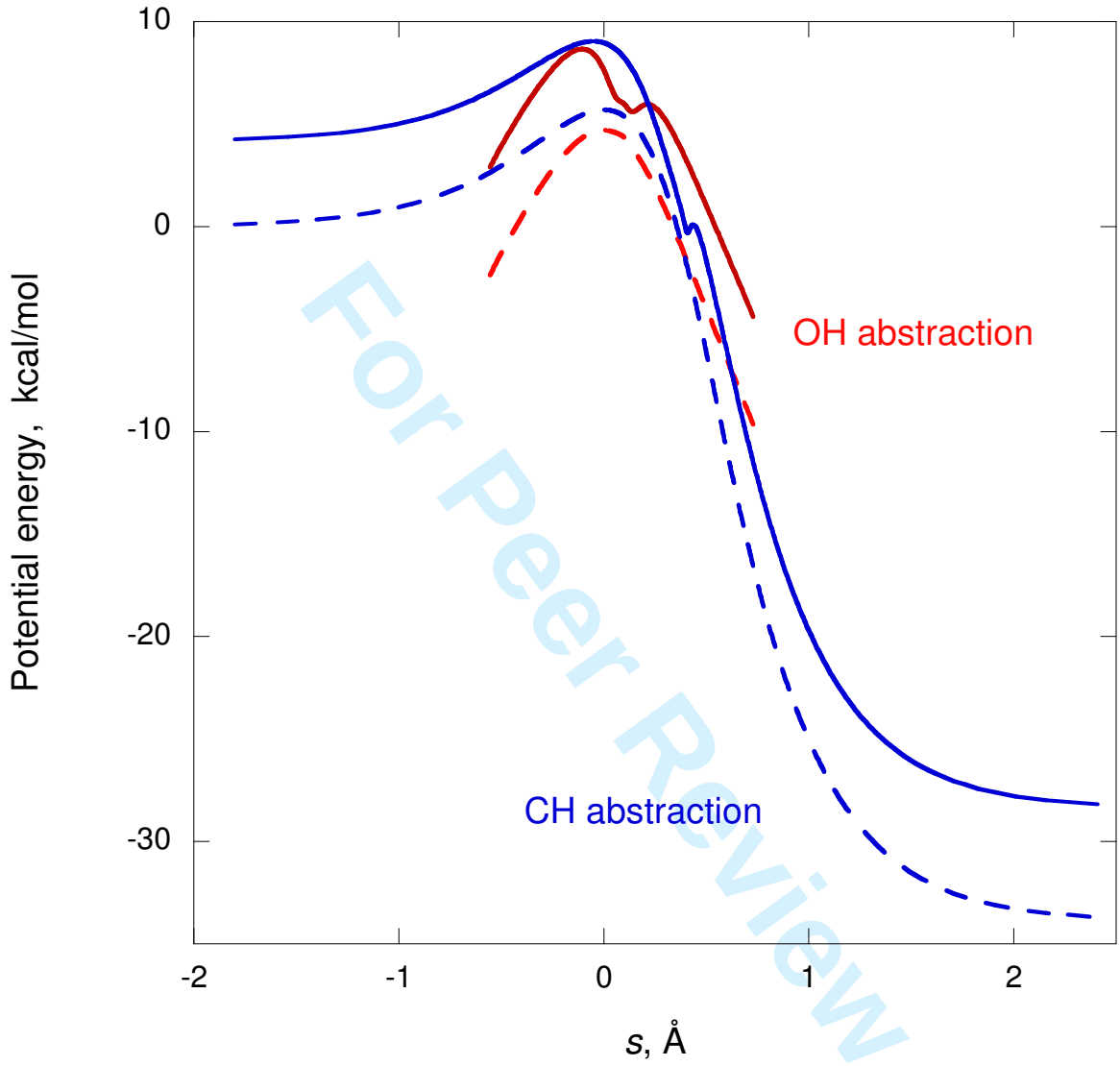

Figure 6. Classical (dashed lines) and vibrationally adiabatic (full lines) reaction paths calculated using ISM/scTST for the H-abstractions from O-H and C-H bonds in 1-phenylethanol

Conclusions

We have addressed the mechanistic challenge of interpreting the inefficiency of the H-abstraction reaction from 1-phenylethanol by acetophenone triplet, which contrasts with the analogous H-abstraction by benzophenone. Competitive H-abstraction from the OH group was invoked in the

literature to explain this observation. The primary product resulting from H-abstraction from the OH group is a triplet α-hydroxy–alkoxy radical pair. However, the absence of products originating from these radicals implies their involvement in a very fast reaction, competitive with the escape from the solvent cage. The literature data on the competition between H-abstractions from CH and OH bonds was complemented with nanosecond laser flash photolysis and photoacoustic calorimetry studies, which provided new kinetic and thermodynamic data. The overall collected data were interpreted with the Intersecting/Interacting-State Model associated with semi-classical TST rate calculations (ISM/scTST).

Although the H-abstraction from the CH bond is 25 kcal/mol more exothermic than that from the OH bond, ISM calculations support with the competitive character of both processes. One of the reasons is associated with higher Parr electrophilicity index *m* for the oxygen-centred radicals with respect to carbon-centred radicals, which lead to a TS stabilization for the higher *m* values. Furthermore, H-bonding along the reaction coordinate also accelerates the transfers of the H-atom between the oxygen atoms. The barrier along this reaction coordinate is relatively narrow and leads to the calculated tunnelling correction of ca. 9. This substantial tunnelling also compensates the loss of exothermicity with respect to the H-abstraction from the CH bond. According to such a view, deuteration of the alcohol reduces the tunnelling correction from ca. 9 to 3, and is the major contributor to the KIE. This emphasizes the role of nuclear tunnelling in the competitive character of the OH and CH abstractions of acetophenone triplet from 1-phenylethanol.

Acknowledgements

We thank Fundação para a Ciência e a Tecnologia (Portugal) e FEDER for financial support; project no. POCI/QUI/55505/2004. MB thanks the financial support by FCT through grant BPD/22070/2005.

References

[1] S. J. Formosinho, L. G. Arnaut, *Adv. Photochem.* **1991**, *16*, 67.
[2] N. J. Turro, *Modern Molecular Photochemistry*, University Sience Books, New York, **1991**.
[3] S. J. Formosinho, *J. Chem. Soc. Faraday Trans. 2* **1976**, *72*, 1313.
[4] S. J. Formosinho, *J. Chem. Soc. Faraday Trans. 2* **1978**, *74*, 1978.
[5] L. G. Arnaut, A. A. C. C. Pais, S. J. Formosinho, M. Barroso, *J. Am. Chem. Soc.* **2003**, *125*, 5236.
[6] M. Barroso, L. G. Arnaut, S. J. Formosinho, *ChemPhysChem* **2005**, *6*, 363.
[7] L. G. Arnaut, S. J. Formosinho, M. Barroso, *J. Mol. Struct.* **2006**, *786*, 207.
[8] M. Barroso, L. G. Arnaut, S. J. Formosinho, *J. Phys. Org. Chem.* **2008**, *21*, 659.
[9] L. G. Arnaut, S. J. Formosinho, *Chem. Eur. J.* **2008**, *14*, 6578.
[10] P. J. Wagner, Q. Cao, R. Pabon, *J. Am. Chem. Soc.* **1992**, *114*, 346.
[11] W. M. Nau, *Ber. Bunsenges. Phys. Chem.* **1998**, *102*, 476.
[12] T. Arai, S. Tobita, H. Shizuka, *J. Am. Chem. Soc.* **1995**, *117*, 3968.
[13] L. G. Arnaut, S. J. Formosinho, A. M. Silva, *J. Photochem. Photobiol. A: Chem* **1984**, *27*, 185.
[14] P. J. Wagner, A. E. Puchalski, *J. Am. Chem. Soc.* **1980**, *102*, 7138.
[15] P. J. Wagner, Y. Zhang, A. Puchalski, *J. Phys. Chem. B* **1993**, *97*, 13368.
[16] F. A. Schaberle, R. M. D. Nunes, M. Barroso, C. Serpa, L. G. Arnaut, **submitted**.
[17] M. Barroso, L. G. Arnaut, S. J. Formosinho, *J. Phys. Chem. A* **2007**, *111*, 591.
[18] L. G. Arnaut, S. J. Formosinho, H. D. Burrows, *Chemical Kinetics*, Elsevier, Amsterdam, **2007**.
[19] L. G. Arnaut, R. A. Caldwell, J. E. Elbert, L. A. Melton, *Rev. Sci. Instrum.* **1992**, *63*, 5381.
[20] L. G. Arnaut, A. A. C. C. Pais, S. J. Formosinho, *J. Mol. Struct.* **2001**, in press.
[21] L. G. Arnaut, S. J. Formosinho, *Chem. Eur. J.* **2007**, *13*, 8018.
[22] M. Barroso, L. G. Arnaut, S. J. Formosinho, *J. Phys. Org. Chem.* **2009**, *22*, 254.
[23] H. S. Johnston, C. Parr, *J. Am. Chem. Soc.* **1963**, *85*, 2544.
[24] L. Pauling, *J. Am. Chem. Soc.* **1947**, *69*, 542.
[25] A. J. C. Varandas, F. B. Brown, C. A. Mead, D. G. Truhlar, B. C. Garrett, *J. Chem. Phys.* **1987**, *86*, 6258.
[26] R. G. Parr, L. v. Szentpály, S. Liu, *J. Am. Chem. Soc.* **1999**, *121*, 1922.
[27] E. B. Wilson Jr., *J. Chem. Phys.* **1939**, *7*, 1047.
[28] B. C. Garrett, D. G. Truhlar, *J. Phys. Chem.* **1979**, *83*, 2921.
[29] S. Glasstone, K. J. Laidler, H. Eyring, *The Theory of Rate Processes*, McGraw-Hill, New York, **1941**.
[30] E. R. Lippincott, R. Schroeder, *J. Chem. Phys.* **1955**, *23*, 1099.
[31] L. G. Arnaut, M. Barroso, D. Oliveira, **2006, University of Coimbra**, http://www.ism.qui.uc.pt:8180/ism/.
[32] H. Lutz, E. Bréhéret, L. Lindqvist, *J. Phys. Chem.* **1973**, *77*, 1758.
[33] H. Lutz, L. Lindvist, *J. Chem. Soc. D* **1971**, 493.
[34] S. L. Murov, I. Carmichael, G. L. Hug, *Handbook of Photochemistry*, 2nd ed., Marcel Dekker, Inc., New York, **1993**.
[35] R. A. Caldwell, S. C. Gupta, *J. Am. Chem. Soc.* **1989**, *111*, 740.
[36] P. Haspra, A. Sutter, J. Wirz, *Angew. Che. Int. Ed. Engl.* **1979**, *18*, 617.
[37] F. Turecek, *Tetrahedron Lett.* **1986**, *27*, 4219.
[38] L. G. Arnaut, R. A. Caldwell, *J. Photochem. Photobiol. A: Chem* **1992**, *65*, 15.
[39] *Handbook of Chemistry and Physics*, 3rd electronic ed., CRC Press Inc., **2001**.
[40] M. Frenkel, K. N. Marsh, R. C. Wilhoit, G. J. Kabo, G. N. Roganov, *Thermodynamics Research Center, College Station, TX* **1994**.

[41] *NIST Chemistry WebBook, NIST Standard Reference Database Number 69, Eds. P.J. Linstrom and W.G. Mallard, http://webbook.nist.gov.*